Materials Science and Engineering C 45 (2014) 89–93

Contents lists available at ScienceDirect

Materials Science and Engineering C

journal homepage: www.elsevier.com/locate/msec

Short communication

Computational study and experimental validation of porous structures fabricated by electron beam melting: A challenge to avoid stress shielding

A. Herrera [a], A. Yánez [a,*], O. Martel [a], H. Afonso [b], D. Monopoli [b]

[a] Department of Mechanical Engineering, University of Las Palmas de Gran Canaria, Spain
[b] Department of Mechanical Engineering, Instituto Tecnológico de Canarias, Spain

ARTICLE INFO

Article history:
Received 28 May 2014
Received in revised form 23 July 2014
Accepted 29 August 2014
Available online 6 September 2014

Keywords:
Electron beam melting
Finite element method
Titanium alloys
Non-stochastic porous structures

ABSTRACT

In this paper, several diamond non-stochastic lattice structures, fabricated by electron beam melting, were mechanically characterized by compression tests. A finite element model of the structures was developed, obtaining an equation that estimates the elastic modulus of the lattice structure. Finally, the differences between the numerical and the experimental results were analyzed and discussed.

1. Introduction

The current therapies for prosthetic joint replacement, in spite of being effective in short-to-medium-term treatments, may be improved with regard to certain characteristics such as stability, functionality, durability, costs and osteointegration, especially in cases of low bone quality. Therefore, it is necessary to find new solutions to integrate the mechanical support function and the regenerative capacity of tissue engineering into a single system.

Recently developed additive manufacturing techniques allow the production of porous titanium biomaterials [1]. The main advantage of these techniques, as compared to others, is their ability to manufacture interconnected porous biomaterials with predictable and predetermined unit cells. This means that the possibility to combine designs of unit cells will open up a broad field with many opportunities for optimal design of orthopedic implants [2]. One of these techniques is the Electron Beam Melting (EBM), developed by Arcam AB (Krokslätts Fabriker 27A, SE-43137 Mölndal, Sweden).

There are certain medical applications, such as the acetabular cups produced in Ti6Al4V by EBM, which have been successfully implemented for years [3]. There is also a wide variety of biomedical implants manufactured with EBM technology that are under investigation, as for example, customized hip and knee implants or bone grafting, including craniofacial and maxillofacial replacements. [4–7]. In many cases, the aim is, on one hand, to fabricate three-dimensional structures with an interconnected porosity suitable for tissue ingrowth and vascularization, and, on the other hand, to search for mechanical properties, such as compressive strength and elastic modulus (E), that are similar to those of human bone. Thus, stress shielding effects after implantation might be avoided [8,9]. However, the mechanical properties of human bone may greatly vary depending on whether it is a cortical or a trabecular bone, or on the quality of the bone, which could be also affected by diseases such as osteoporosis. Therefore, the current trend is to fabricate patient-tailored implants for which some researchers have proposed finite element (FE) models for the evaluation of porous titanium (Ti6Al4V) structures for biomedical applications in order to optimize designs [2,5,10,11].

There are many types of non-stochastic lattice structures that could meet the above-mentioned objectives [6,12–14]. In this study, diamond structures, based on the CAD model for diamond lattice structures (Fig. 1.), have been modeled and manufactured by the EBM method. Previously, other authors have also focused on the study of the mechanical properties of diamond lattice unit cells by experimental, numerical and analytical methods [15].

The aim of this article was to fabricate non-stochastic lattice structures by EBM method to examine the mechanical properties under compression load and to compare them both with the results obtained by the FE method and with the properties of human bone. The final objective was the characterization of porous structures in order to

* Corresponding author. Tel.: +34 619 28 88 61; fax: +34 928 45 14 84.
E-mail address: myanez@dim.ulpgc.es (A. Yánez).

http://dx.doi.org/10.1016/j.msec.2014.08.050
0928-4931/

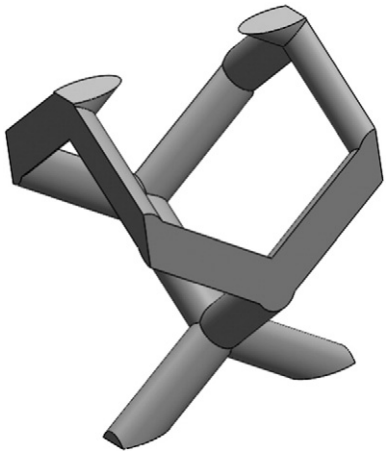

Fig. 1. CAD model of the base cell of the structure used.

obtain FE models permitting the study and optimization of the design of medical applications without the need to previously test or manufacture.

2. Experimental procedure

Several specimens were designed in Pro/ENGINEER Wildfire 4.0 (PTC, MA) and manufactured by EBM techniques. The general procedure for the component generation layer by layer has already been described by other authors [8,13,14,16]. Titanium powders (Ti6Al4V) were used as raw material. The material properties were assumed to be linear isotropic with an elastic modulus of 110 GPa and a Poisson's ratio of 0.3. Mechanical testing of the bulk material according to ASTM E8M-13a Standard Test Methods for Tension Testing of Metallic Materials confirms these assumptions. The maximum acceptable build angle without losing mechanical properties has been taken into account. If the angle is too small, the overlap between each layer is insufficient and the strength achieved is poor [17]. According to experimental tests conducted with Arcam AB technology, a minimum build angle of 20° has been established to avoid failure [12]. However, the size of the powder does not significantly influence the final mechanical properties of the specimens [18].

The specimens were diamond-like structures with nominal cell sizes of 1.5 mm, 2.5 mm and 4 mm, nominal strut diameters of 0.5 mm, 0.6 mm, 0.7 mm and 1.0 mm, and several aspect ratios, making a total of 8 different types of specimens (Table 1). The size of the struts was measured using a stereomicroscope Olympus SZX10 (Olympus Corporation, Tokyo, Japan). The measurements were processed with specific microscope software in order to obtain the diameter of the struts and the size of the pores. The strut diameter and pore size measured values differ less than 10% from the nominal value.

In order to perform adequate mechanical tests and avoid unwanted stress distributions, the flatness of the upper and lower sides was verified, rectifying defects greater than 1° by surface machining, obtaining geometries as shown in Fig. 2.

Uniaxial compression tests were conducted at a speed of 0.5 mm/min according to ASTM E9-09 Standard Test Methods of Compression Testing. The upper head was articulated and the load was applied onto the plain plate placed on the upper and lower sides of the specimen. All the specimens were loaded until failure. Five samples of each type of structure have been taken ($n = 5$). Fig. 3 shows the typical curve of stress versus strain obtained in compression tests. Both stress and strain were obtained in accordance with the initial cross sectional area and the initial length of each structure, respectively. The stiffness of each specimen was named as E value and was obtained as the gradient of the most linear part of each curve, as shown in Fig. 3.

For the FE studies, specimens were modeled using Pro/ENGINEER Wildfire 4.0 (PTC, MA) and subsequently analyzed using Abaqus 6.9.1 software (Dassault Systèmes SIMULIA). Due to the geometric complexity of the structure, the type of element selected for the mesh was C3D4 after conducting the relevant sensitivity tests. To simulate the boundary conditions of the compression test, the lower side was fixed in all the structures and a displacement of 0.1 mm was applied to the upper side.

Table 1
Structure identification and dimensions of the specimens tested. D: Strut diameter. S: Cell size.

Structure	Dimensions (mm)	D (mm)	S (mm)	Aspect ratio (S/D)
(a)	21.0 × 21.0	0.7	4.0	5.71
(b)	38.0 × 29.0	0.7	4.0	5.71
(c)	25.0 × 19.0	0.6	2.5	4.17
(d)	21.0 × 21.0	1.0	4.0	4.00
(e)	39.0 × 20.0	0.7	2.5	3.57
(f)	16.5 × 12.5	0.5	1.5	3.00
(g)	29.0 × 22.0	1.0	2.5	2.50
(h)	18.0 × 14.0	0.7	1.5	2.14

3. Results and discussion

Fig. 4 shows the mean and standard deviation of elastic modulus (E), as well as the aspect ratio obtained from the eight types of specimens tested. As shown in the figure, the lower the aspect ratio is, the higher the E value is. Furthermore, in structures *a* and *d*, which have the same aspect ratio, the E value is statistically the same. The structure dimensions did not seem to have influence on the E values. The reduced standard deviation values demonstrate the accuracy of the manufacturing technique.

The compression tests showed a wide range of E values between 407.8 MPa and 12,228.8 MPa. Those values are within the E range for human bone tissue, both for cancellous bone (100–1500 MPa) and cortical bone (12000–18000 MPa) [19–21]. This fact reveals that this fabrication technique, in contrast with manufacturing processes that result in stochastic lattice structures, is suitable not only to develop structures with mechanical properties similar to the trabecular bone, but also to develop cortical bone-like structures [22].

The FE studies reached satisfactory results when comparing the data obtained in the compression tests. The mean and standard deviation of the percentages of difference between the compression test values and the FE values are 27.5 ± 3.1% (Table 2). This small standard deviation means that the relative differences in the E values between the compression tests and the FE results are similar in each type of structure (Fig. 5). Eq. (1) estimates the elastic modulus (E in MPa) obtained with FE methods related to the aspect ratio (S/D). The inverse relationship between E and aspect ratio is shown again.

$$E = 221082\left(\frac{S}{D}\right)^{-3.411}. \quad (1)$$

The differences between the FE method and the compression tests are not attributable to a single parameter, but to several of them. Surface roughness or variations in the strut area randomly produced in the manufacturing process are not found in the FE model. Those irregularities frequently generate stress concentrators that could affect the mechanical behavior, so the properties obtained by simulation are higher than those obtained in the compression tests [4,23,24]. If the manufacturing parameters are not properly adjusted, void spaces or unmelted material may be generated (Fig. 6), which might reduce the mechanical properties. Also, deficiencies in the fabrication could mean that the struts might not be perfectly straight, which would cause a loss of stiffness. The size of the specimen becomes a critical

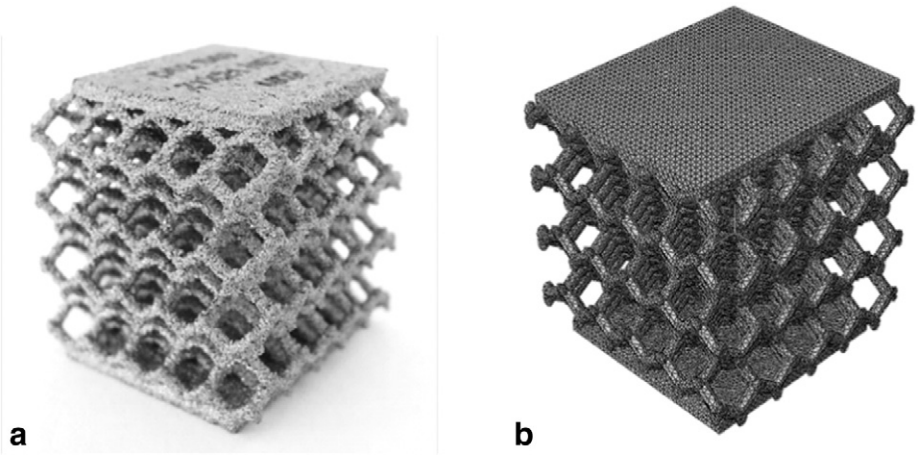

Fig. 2. Example of specimen used to determine its mechanical properties (a) next to an identical 3D model for calculation in FE (b).

factor in the case of having small dimensions since a broken strut may lead to the complete failure of the structure due to a higher influence of the elastic instability phenomena [25]. The anisotropy of the specimens affects the agreement of the results in such a way that the divergence grows proportionally to the directional dependence of the elastic modulus [26]. Some of those imperfections, inherent to the manufacturing process, might be improved by heat treatment [10,27]. On the other hand, Campoli et al. have implemented the irregularities in the FE model with better results than those obtained from analytical models [2]. Those irregularities have not been implemented in our case.

Another limitation in this study was its focus on diamond structures. However, there are multiple non-stochastic lattice structures which could provide satisfactory results in order to reduce the stress shielding phenomenon, without decreasing the appropriate mechanical support. Some of them, such as auxetic, cubic, rhombic dodecahedron and truncated octahedron structures, have already been studied by other authors, obtaining satisfactory results [2,8,11,13,14,16].

Another of the critical points of this study is the diversity of the pore size of the geometries studied. It is known that interconnected porous structures with pore diameters between 100 μm and 400 μm are required to facilitate cell migration, tissue ingrowth and vascularization [8,28,29], although some researchers have also pointed that bone ingrowth successfully covers pore sizes up to 2 mm [30]. Despite the fact that the cell sizes of the structures, studied in this research, range from 1.5 mm to 4 mm, with the biggest pore size far from the optimal distance observed for tissue regeneration, several techniques can be applied to increase and facilitate tissue ingrowth inside the geometry. Surface modifications like wet chemical treatment in HCl and NaOH can increase the osteointegration and tissue growth [8]. Additional strategies can also cover collagen type I and hydroxyapatite coatings or the inclusion of biopolymers inside the structure to facilitate the first stages of cell adhesion and tissue formation without a major modification of the mechanical properties that are aiming to mimic those of the bone [13,31–34].

4. Conclusions

In this study, diamond non-stochastic lattice structures were characterized by carrying out FE studies and subsequent validation with compression tests of specimens fabricated by EBM. The values obtained are considered satisfactory in that the difference between the FE results and the compression tests is established in relatively stable and predictable figures. The possible causes for the differences between the FE results and the compression tests have been discussed in this paper. In order to design optimal orthopedic implants, the phenomena causing those differences must be implemented in FE models.

Once those factors are characterized, computational models can be performed with no need to fabricate real components to be used in experimental testing to verify their properties. That would therefore be an inexpensive, quick and customized solution to a large number of patients, and would also enable speeding up the process from the

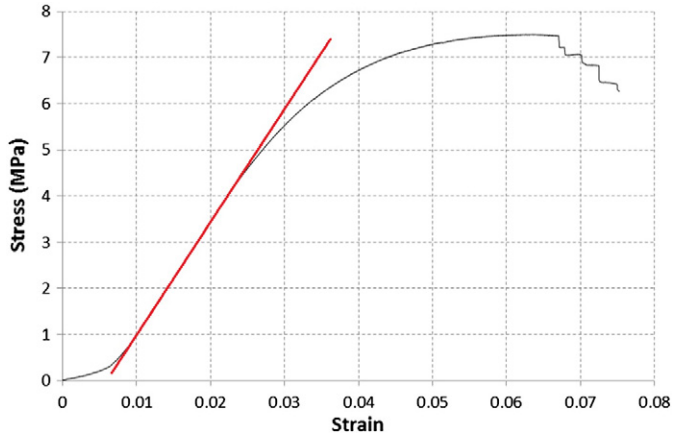

Fig. 3. Stress–strain curve obtained in compression tests for a D07 S40 structure. The straight line represents the line used to estimate the E value.

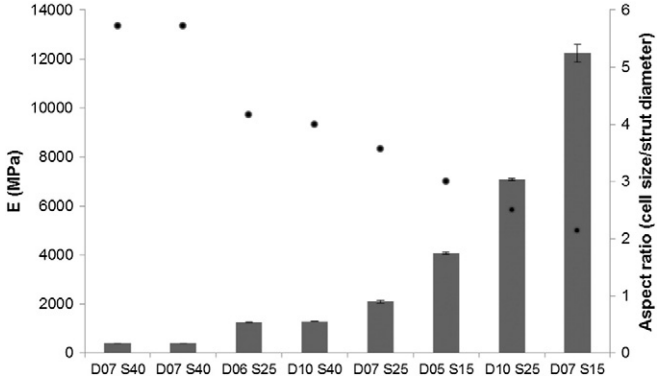

Fig. 4. Elastic moduli obtained by compression tests (dark gray bars) and relationship between the cell size and the strut diameter (black dots). D and S represent strut diameter and cell size, respectively.

Table 2
Comparison between the elastic moduli obtained by finite elements and the compression tests (mean and standard deviation).

Structure	E (MPa) (Abaqus)	E (MPa) (compression test)		Difference (%)
(a)	542.9	407.8 ± 3.8		24.9
(b)	603.0	407.1 ± 5.3		32.5
(c)	1780.1	1259.6 ± 10.5		29.2
(d)	1837.6	1304.8 ± 13.0		29.0
(e)	2997.4	2096.6 ± 61.4		30.1
(f)	5451.8	4078.6 ± 47.5		25.2
(g)	9306.3	7078.8 ± 45.1		23.9
(h)	16319.7	12228.8 ± 375.8		25.1
			$\bar{x}$	27.5
			σ	3.1

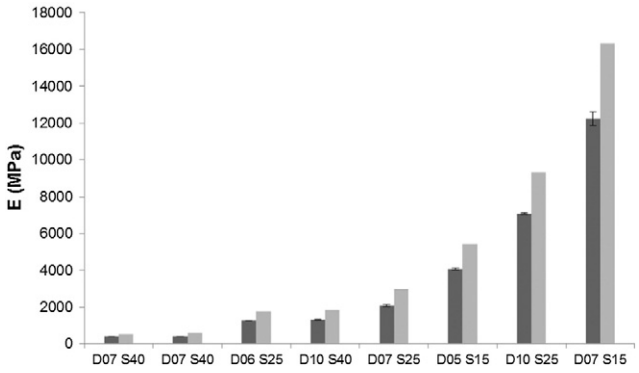

Fig. 5. Elastic moduli obtained by finite elements (light gray bar) and comparison to those obtained by compression tests (dark gray bar). D and S represent diameter and strut dimensions, respectively.

moment that the need for intervention arises until the repair is completed, a especially critical factor in cases of catastrophic damage. Hence, it would be possible to design the type of structure that best suits the needs of each patient's bone according to the mechanical forces that the joint will subsequently experience.

In addition to the above, it would also be necessary to conduct fatigue testing, study other types of structures, perform studies of implant models with this type of structure, and either conduct surface modifications or fill the void pores spaces with biodegradable polymers or bioceramics in order to improve cell growth.

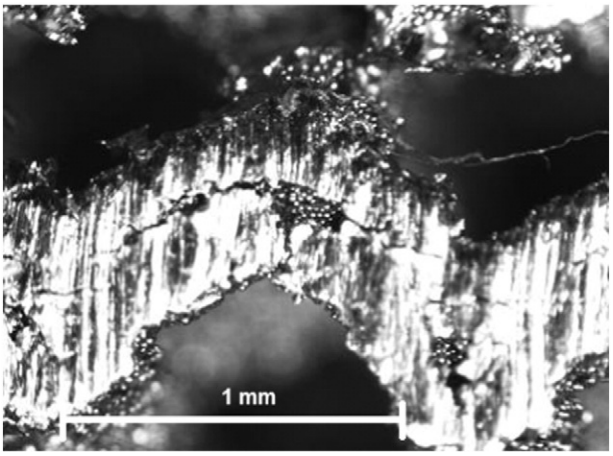

Fig. 6. Structure incorrectly fabricated due to a lack of melting in one of the struts. Unmelted powder can be observed. Image obtained with stereomicroscope Olympus SZX10.

Acknowledgments

The authors gratefully acknowledge the help with the Abaqus FE calculations from the University of Malaga Mechanical Engineering Department (Spain).

References

[1] R. Singh, P.D. Lee, R.J. Dashwood, T.C. Lindley, Titanium foams for biomedical applications: a review, Mater. Technol. 25 (2010) 127–136.
[2] G. Campoli, M.S. Borleffs, S. Amin Yavari, R. Wauthle, H. Weinans, A.A. Zadpoor, Mechanical properties of open-cell metallic biomaterials manufactured using additive manufacturing, Mater. Des. 49 (2013) 957–965.
[3] S. Thundal, Rapid manufacturing of orthopaedic implants, Adv. Mater. Process. 166 (2008) 60–62.
[4] M. Cronskär, L. Rännar, M. Bäckström, Production of customized hip stem prostheses — a comparison between conventional machining and electron beam melting (EBM), Rapid Prototyp. J. 19 (2013) 365–372.
[5] O.L.A. Harrysson, O. Cansizoglu, D.J. Marcellin-Little, D.R. Cormier, H.A. West II, Direct metal fabrication of titanium implants with tailored materials and mechanical properties using electron beam melting technology, Mater. Sci. Eng. C 28 (2008) 366–373.
[6] L.E. Murr, S.M. Gaytan, F. Medina, H. Lopez, E. Martinez, B.I. Machado, D.H. Hernandez, L. Martinez, M.I. Lopez, R.B. Wicker, J. Bracke, Next-generation biomedical implants using additive manufacturing of complex cellular and functional mesh arrays, Philos. Trans. R. Soc. 368 (2010) 1999–2032.
[7] L.E. Murr, S.M. Gaytan, E. Martinez, F. Medina, R.B. Wicker, Next generation orthopaedic implants by additive manufacturing using electron beam melting, Int. J. Biomater. (2012) ID 245727.
[8] P. Heinl, L. Müller, C. Körner, R.F. Singer, F.A. Müller, Cellular Ti-6Al-4V structures with interconnected macro porosity for bone implants fabricated by selective electron beam melting, Acta Biomater. 4 (2008) 1536–1544.
[9] X. Li, C. Wang, W. Zhang, Y. Li, Fabrication and characterization of porous Ti6Al4V parts for biomedical applications using electron beam melting process, Mater. Lett. 63 (2009) 403–405.
[10] B. Gorny, T. Niendorf, J. Lackmann, M. Thoene, T. Troester, H.J. Maier, In situ characterization of the deformation and failure behavior of non-stochastic porous structures processed by selective laser melting, Mater. Sci. Eng. A 528 (2011) 7962–7967.
[11] M. Smith, Z. Guan, W.J. Cantwell, Finite element modelling of the compressive response of lattice structures manufactured using the selective laser melting technique, Int. J. Mech. Sci. 67 (2013) 28–41.
[12] O. Cansizoglu, O. Harrysson, D. Cormier, H. West, T. Mahale, Properties of Ti-6Al-4V non-stochastic lattice structures fabricated via electron beam melting, Mater. Sci. Eng. A 492 (2008) 468–474.
[13] J. Parthasarathy, B. Starly, S. Raman, A. Christensen, Mechanical evaluation of porous titanium (Ti6Al4V) structures with electron beam melting (EBM), J. Mech. Behav. Biomed. Mater. 3 (2010) 249–259.
[14] L. Yang, D. Cormier, H. West, O. Harrysson, K. Knowlson, Non-stochastic Ti-6Al-4V foam structures with negative Poisson's ratio, Mater. Sci. Eng. A 558 (2012) 579–585.
[15] S.M. Ahmadi, G. Campoli, S. Amin Yavari, B. Sajadi, R. Wauthle, J. Schrooten, H. Weinans, A.A. Zadpoor, Mechanical behavior of regular open-cell porous biomaterials made of diamond lattice unit cells, J. Mech. Behav. Biomed. Mater. 34 (2014) 106–115.
[16] P. Heinl, C. Körner, R.F. Singer, Selective electron beam melting of cellular titanium: mechanical properties, Adv. Eng. Mater. 10 (2008) 882–888.
[17] O. Cansizoglu, O.L.A. Harrysson, H.A. West II, D.R. Cormier, T. Mahale, Applications of structural optimization in direct metal fabrication, Rapid Prototyp. J. 14 (2008) 114–122.
[18] J. Karlsson, A. Snis, H. Engqvist, J. Lausmaa, Characterization and comparison of materials produced by Electron Beam Melting (EBM) of two different Ti-6Al-4V powder fractions, J. Mater. Process. Technol. 213 (2013) 2109–2118.
[19] A.H. Burstein, D.T. Reilly, M. Martens, Aging of bone tissue: mechanical properties, J. Bone Joint Surg. Am. 58 (1976) 82–86.
[20] D.T. Reilly, A.H. Burstein, V.H. Frankel, The elastic modulus for bone, J. Biomech. 7 (1974) 271–275.
[21] D.T. Reilly, A.H. Burstein, The elastic and ultimate properties of compact bone tissue, J. Biomech. 8 (1975) 393–405.
[22] L.E. Murr, S.M. Gaytan, F. Medina, E. Martinez, J.L. Martinez, D.H. Hernandez, B.I. Machado, D.A. Ramirez, R.B. Wicker, Characterization of Ti-6Al-4V open cellular foams fabricated by additive manufacturing using electron beam melting, Mater. Sci. Eng. A 527 (2010) 1861–1868.
[23] S. Van Bael, G. Kerckhofs, M. Moesen, G. Pyka, J. Schrooten, J.P. Kruth, Micro-CT-based improvement of geometrical and mechanical controllability of selective laser melted Ti6Al4V porous structures, Mater. Sci. Eng. A 528 (2011) 7423–7431.
[24] C.Y. Lin, T. Wirtz, F. LaMarca, S.J. Hollister, Structural and mechanical evaluations of a topology optimized titanium interbody fusion cage fabricated by selective laser melting process, J. Biomed. Mater. Res. A 83 (2007) 272–279.
[25] E. Marin, S. Fusi, M. Pressacco, L. Paussa, L. Fedrizzi, Characterization of cellular solids in Ti6Al4V for orthopaedic implant applications: trabecular titanium, J. Mech. Behav. Biomed. Mater. 3 (2010) 373–381.
[26] M.H. Luxner, J. Stampfl, H.E. Pettermann, Linear and nonlinear numerical investigations of regular open cell structures, Proc. IMECE2004 ASME, 2004, (IMECE2004-62545).

[27] G. Lütjering, Influence of processing on microstructure and mechanical properties of (a + ß) titanium alloys, Mater. Sci. Eng. A 243 (1998) 32–45.
[28] C.A. van Blitterswijk, J.J. Grote, W. Kuijpers, W.T. Daems, K. de Groot, Macropore tissue ingrowth: a quantitative and qualitative study on hydroxyapatite ceramic, Biomaterials 7 (1986) 137–143.
[29] H. Schliephake, F.W. Neukam, D. Klosa, Influence of pore dimensions on bone ingrowth into porous hydroxylapatite blocks used as bone graft substitutes. A histometric study, Int. J. Oral Maxillofac. Surg. 20 (1991) 53–58.
[30] J.D. Bobyn, R.M. Pilliar, H.U. Cameron, G.C. Weatherly, The optimum pore size for the fixation of porous surfaced metal implants by the ingrowth of bone, Clin. Orthop. 150 (1980) 263–270.
[31] M. Alonso, S. Claros, J. Becerra, J.A. Andrades, The effect of type I collagen on osteochondrogenic differentiation in adipose-derived stromal cells in vivo, Cytotherapy 10 (2008) 597–610.
[32] J.R. Cano, L. Santos-Ruiz, E. Guerado, J. Becerra, Osteoprogenitor cell adhesiveness to a titanium mesh. A clinically relevant hypothesis for revision surgery in hip replacement, Hip Int. 20 (Suppl. 7) (2010) S102–S105.
[33] J. Isaac, A. Galtayries, T. Kizuki, T. Kokubo, A. Berda, J.M. Sautier, Bioengineered titanium surfaces affect the gene-expression and phenotypic response of osteoprogenitor cells derived from mouse calvarial bones, Eur. Cell. Mater. 20 (2010) 178–196.
[34] S. Piskounova, J. Forsgren, U. Brohede, H. Engqvist, M. Strømme, In vitro characterization of bioactive titanium dioxide/hydroxyapatite surfaces functionalized with BMP-2, J. Biomed. Mater. Res. Part B Appl. Biomater. 91 (2009) 780–787.